

Low-stress and high-reflectance Mo/Si multilayers for extreme ultraviolet lithography by magnetron sputtering deposition with bias assistance

Bo Yu,* Chunshui Jin, Shun Yao, Chun Li, Yu Liu, Feng Zhou, Benyin Guo, Hui Wang, Yao Xie, and Liping Wang

State Key Laboratory of Applied Optics, Changchun Institute of Optics and Fine Mechanics, Chinese Academy of Sciences, Changchun 130033, China

*Corresponding author: yubo@ciomp.ac.cn

Received 31 May 2017; revised 6 August 2017; accepted 21 August 2017; posted 21 August 2017 (Doc. ID 296875); published 8 September 2017

To explore the potential of achieving low-stress and high-reflectance Mo/Si multilayers deposited by conventional magnetron sputtering with bias assistance, we investigated the effects of varying Ar gas pressure, substrate bias voltage, and a bias-assisted Si ratio on the stress and extreme ultraviolet (EUV) reflectance of Mo/Si multilayers. To reduce the damage of ion bombardments on an Si-on-Mo interface, only the final part of the Si layer was deposited with bias assistance. Bias voltage has strong influence on the stress. The compressive stress of Mo/Si multilayers can be reduced remarkably by increasing bias voltage due to the increase of Mo-on-Si interdiffusion and postponement of Mo crystallization transition. Properly choosing gas pressure and a bias-assisted Si ratio is critical to obtain high EUV reflectance. Appropriately decreasing gas pressure can reduce the interface roughness without increasing interdiffusion. Too much bias assistance can seriously reduce the optical contrast between Mo and Si layers and lead to a remarkable decrease of EUV reflectance. Thus, by appropriately choosing gas pressure, bias voltage, and a bias-assisted Si ratio, the stress values of Mo/Si multilayers can be reduced to the order of -100 MPa with an EUV reflectance loss of about 1%. © 2017 Optical Society of America

OCIS codes: (340.7480) X-rays, soft x-rays, extreme ultraviolet (EUV); (310.0310) Thin films; (230.4170) Multilayers; (340.0340) X-ray optics.

<https://doi.org/10.1364/AO.56.007462>

1. INTRODUCTION

Extreme ultraviolet (EUV) lithography at an operation wavelength of 13.5 nm is the main candidate for next generation lithography. As EUV radiation is strongly absorbed by all materials and the refractive index of the materials is so close to unity, optical refractive elements cannot be used in EUV lithography optical systems, and therefore an all-reflective optical system is essential. To improve the reflectivity, high reflective normal incidence Mo/Si multilayer coatings need to be deposited on optics. Mo/Si multilayers can be deposited by different methods, including magnetron sputtering [1–4], electron beam evaporation [5,6], ion beam sputtering [7,8], and pulsed laser deposition [9]. Among them, the most commonly used is magnetron sputtering. The advantages of this technique are the stability of the sources, reproducibility from run to run, relatively fast deposition rate, and the ability to coat large optics with a high-precision lateral thickness profile [10].

However, it is known that high-reflective Mo/Si multilayer coatings deposited by magnetron sputtering develop compressive stresses of 400 MPa to 500 MPa [11,12], which are large enough to deform the precisely figured substrates [13]. Therefore, it is important to develop suitable methods to negate the effects of the stress without significantly reducing the EUV reflectivity. To reduce Mo/Si multilayer film stress to an acceptable level, several techniques can be applied. First, it is known that a larger Mo fraction (Γ) in Mo/Si multilayers shifts the stress from a compressive to a more tensile stress. So, the stress in Mo/Si multilayer coatings can be easily tuned to zero by an appropriate adjustment of Γ . However, in this case, the EUV reflectivity loss is more than 20%, which is unacceptable for an EUV lithography tool [14]. Second, postdeposition annealing is also an effective method for stress relaxation in Mo/Si multilayer coatings. It was shown previously by Mirkarimi and Montcalm [12] that a 75% reduction in stress with a relatively

small decrease of 1.3% in EUV reflectance can be achieved by annealing the Mo/Si multilayer structure at 200°C. However, the approach can be used only for EUV optics tolerant to thermal treatment. Another option is to compensate compressive stress by a single buffer layer or secondary multilayer film with opposite stress underneath the high-reflectance multilayer. For instance, Shiraishi *et al.* [15] fabricated double-stacked Mo/Si multilayers, in which a reflective block of a compressive Mo/Si multilayer was deposited on a stress-compensating block of tensile Mo/Si multilayer. The compressive stress of multilayer coatings was reduced from 400 MPa to 6 MPa with an EUV reflectance loss of nearly 2%. The disadvantage of double-stacked Mo/Si multilayers is that the thick stress-compensating multilayer increases the multilayer-added figure error significantly, something undesirable for EUV optics with stringent figure error tolerances. A single buffer layer with several tens of nanometers can also be used to compensate for the compressive stress of a high-reflectance Mo/Si multilayer, as reported by Soufli *et al.* [16]. The multilayer coatings that they developed for MET5 projection optics consisted of 30-pair Mo/Si multilayers with the Γ ratio of 0.47 and contained a 27.9-nm-thick Cr underlayer. The resulting multilayer coating stress values were on the order of -100 MPa (compressive), and the EUV reflectance loss was nearly 4%, which was caused by the relatively high surface roughness of the Cr underlayer and the use of a relatively large Γ ratio. It should be emphasized that all the multilayer coatings mentioned above were deposited by magnetron sputtering without ion assistance. The additional use of ions during or after the deposition allows wider process latitude for stress optimization under the boundary condition of minimal loss of reflectance and minimal multilayer-added figure error. Yakshin *et al.* [17] developed a new magnetron sputtering deposition system, which was based on the thermal particle features typical for e-beam deposition. In their system, the distance between the substrate and the magnetron source was kept substantially larger than in conventional magnetrons, and by modulating the working gas pressure the magnetron sputtering could work either in the low energy mode or in the high energy mode. Additionally, an extra ion source with a wide energy range was used to gain more flexibility in controlling the energy during different stages of layer growth. The stress of highly reflective Mo/Si multilayers deposited by their system was as low as about -180 MPa. Their results show the practicability to achieve high-reflectance Mo/Si multilayers with stress values on the order of -100 MPa by carefully controlling the energy during different stages of layer growth. In conventional magnetrons, the simplest way to achieve ion bombardment on the growing film and therefore to improve flexibility of controlling the layer growth energy is substrate biasing. The influence of substrate biasing on the growth of Mo/Si multilayers has been investigated by several researchers

[18–20]. In their studies, the substrate bias was applied during the growth of silicon layers to reduce the interface roughness and therefore to improve the reflectivity of Mo/Si multilayers. However, few studies, to our knowledge, have focused on the effects of substrate biasing on the stress of Mo/Si multilayers.

In this work, the potential of achieving low-stress and high-reflectance Mo/Si multilayers deposited by conventional magnetron sputtering with bias assistance was explored. The influence of varying Ar gas pressure, substrate bias voltage, and a bias-assisted Si ratio on the stress and reflectance of Mo/Si multilayers was investigated.

2. EXPERIMENTAL

Mo/Si multilayer coatings with 50 bilayer pairs (periods) were deposited onto superpolished Si (100) substrates with a root mean squared (rms) surface roughness of 0.1 nm by a commercial DC magnetron sputtering system Nussy 1900 from Leybold Optics. In the system, six rectangular sputter sources are radially arranged in a horizontal circular chamber. The substrates are held face up on a rotating table (platter) below the sources. The multilayers are deposited by sweeping the substrates across the sources with controlled rotation of the platter. One bilayer is deposited for each complete revolution of the platter. The layer thicknesses are determined by the time the substrate is exposed to the source, depending on the substrate transit velocity. Additionally, the substrates are rapidly spun about their own optical axis for azimuthal uniformity. During the deposition, a bias voltage can also be applied to the substrate and controlled according to the rotation angle of the substrate. The typical peak reflectance of Mo/Si multilayer coatings (50 periods) deposited by this system is $\sim 68.5\%$, with the compressive stress of ~ 500 MPa. The process gas is Ar, and the sputtering pressure is $8\text{E-}4$ mbar. The Mo and Si sources are operated at powers of 1000 W and 2500 W, respectively. In this study, Mo/Si multilayers were deposited using one Mo source and two Si sources. Relatively high process gas (Ar) pressures were used to thermalize the sputtered atoms or to decrease the energy of the atoms. The initial part of the Si layer was deposited using the first Si source and the final part of the Si layer was deposited using the second Si source. When the substrate swept across the second Si source, a negative bias was applied to provide additional ion bombardment on the growing layer. Therefore, the Mo layer and the initial part of the Si layer were deposited with relatively low energy, whereas the final part of the Si layer was deposited with relatively high energy. Multilayer samples were produced by varying process gas pressure, bias voltage, and ratio of Si layer grown with bias assistance, as presented in Table 1.

The multilayers were analyzed by grazing incidence *x*-ray reflectivity (GIXRR), diffuse scattering measurements, and

Table 1. Process Parameters of Mo/Si Multilayers

Sample ID	M1	M2	M3	M4	M5	M6	M7	M8
Gas pressure, mbar	4.5E-3	3.1E-3	1.8E-3	1.0E-3	1.8E-3	1.8E-3	1.8E-3	1.8E-3
Bias potential, V	-350	-350	-350	-350	-250	-150	-350	-350
Bias-assisted Si ratio	50%	50%	50%	50%	50%	50%	25%	75%

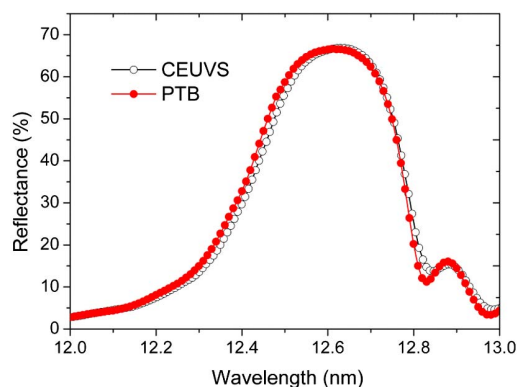


Fig. 1. Reflectance of a Mo/Si multilayer mirror measured with the CEUVS (open circles) and at PTB (closed circles) as the average of the values for *S*- and *P*-polarized radiation.

wide angle *x*-ray diffraction (WAXRD) with a PANalytical X'Pert PRO MRD *x*-ray diffractometer, using Cu-K α line radiation (0.154 nm). During the WAXRD measurements, the sample was aligned with the incident beam at a fixed angle of $\omega = 1^\circ$ to maximize the illuminated area and thereby the diffracted intensity. The period thickness and Γ ratio of Mo/Si multilayers were determined by fitting the GIXRR using a two-layer model without considering the molybdenum silicide layers in Mo-Si interfaces.

In addition to Cu-K α reflectometry and diffractometry, EUV reflectance measurements were carried out by a stand-alone EUV laboratory reflectometer CEUVS designed by Bruker ASC. The comparison of EUV reflectance measurements of Mo/Si multilayer at CEUVS and at the PTB soft *x*-ray radiometry beamline is shown in Fig. 1. The measurements were performed at an angle of incidence 6° with unpolarized radiation at the CEUVS and in *S* and *P* orientation at PTB. Compared to reference measurements at PTB, the peak reflectance difference is smaller than 0.5%, and the wavelength difference is smaller than 0.01 nm.

The curvature of a 4-inch (100 mm) diameter Si wafer was measured before and after coating by a Zygo GPI XP/D interferometer. Then, the film stress can be calculated by Stoney equation [21],

$$\sigma = \frac{E_s}{6(1-\nu_s)} \frac{t_s^2}{t_f} \left(\frac{1}{R} - \frac{1}{R_0} \right), \quad (1)$$

where E_s is Young's elastic modulus of the substrate; ν_s is Poisson's ratio of the substrate; t_s and t_f are the thicknesses of the substrate and film, respectively; and R_0 and R are the radii of curvature of the substrate before and after coating. The quantity $[E_s/(1-\nu_s)]$ for Si (100) was taken as 180 GPa [22].

Transmission electron microscope (TEM) measurements were performed at Materials Analysis Technology Inc. The samples for the TEM analysis were prepared by focused ion beam milling with the use of an FEI Helios instrument. The high-resolution transmission electron microscopy (HRTEM) analyses were performed using an FEI Talos F200X instrument with 0.1 nm resolution. To study the chemical composition variation with the depth of the Mo/Si multilayers, energy

dispersive *x*-ray spectroscopy (EDX) was performed with the same FEI Talos F200X instrument used for TEM. A well-focused electron beam fell normally onto the multilayer cross-section and moved along it perpendicular to interfaces. Characteristic fluorescent radiation of different chemical elements was recorded, allowing the composition distribution of chemical elements in depth of a multilayer structure to be determined. An essential shortcoming of the EDX technique is the impossibility to determine the absolute value of atomic concentration without comparison of the registered signal to that of an etalon sample. At the same time, relative variation in the concentration of the same chemical element is adequately determined by the EDX, sufficient for our study.

3. RESULTS AND DISCUSSION

A. Influence of Gas Pressure on the Reflectance and Stress

Sample M1–M4 were produced by varying Ar gas pressure. A substrate bias of -350 V was applied in the final 50% of the Si layer deposition. The properties of these samples are summarized in Table 2. Owing to the low deposition energy of the Mo layer and the initial part of the Si layer as well as the application of -350 V substrate bias potential during deposition of the final part of the Si layer, Mo/Si multilayers with stress values on the order of -100 MPa were achieved. The variation of gas pressure has limited influence on the stress, whereas it has notable influence on the EUV reflectance of multilayers. As gas pressure decreases from $4.5\text{E-}3$ to $1.8\text{E-}3$ mbar, the peak EUV reflectance increases from 65.4% to 67.1%. A further decrease in the gas pressure does not result in a higher peak EUV reflectance. Figure 2 shows diffuse *x*-ray scattering from Mo/Si multilayers deposited with different Ar gas pressures. The decreased diffuse scattering indicates continuously decreased interface roughness for lower Ar gas pressures. However, the EUV reflectance does not show continuous increase when the Ar gas pressure decreases from $1.8\text{E-}3$ to $1.0\text{E-}3$ mbar. This can be explained by the effect of Ar gas pressure on the interlayer diffusion in Mo/Si multilayers [23]. Too much reduction of gas pressure leads to an obvious increase of interdiffusion, offsetting the positive impact of decreasing interface roughness on the EUV reflectance.

B. Influence of Bias Voltage on the Reflectance and Stress

Samples M5 and M6 were produced by varying substrate bias voltage relative to sample M3. The applied substrate bias voltages in the final 50% of the Si layer deposition were -250 V and -150 V, respectively. The properties of these samples are summarized in Table 3. The variation of bias voltage has little

Table 2. Properties of Samples M1–M4

	Pressure (mbar)	Period Thickness (nm)	Γ	EUV Reflectance (%)	Stress (MPa)
M1	4.5E-3	6.926	0.41	65.4	-121
M2	3.1E-3	6.925	0.40	66.6	-131
M3	1.8E-3	6.940	0.37	67.1	-135
M4	1.0E-3	6.951	0.37	66.8	-160

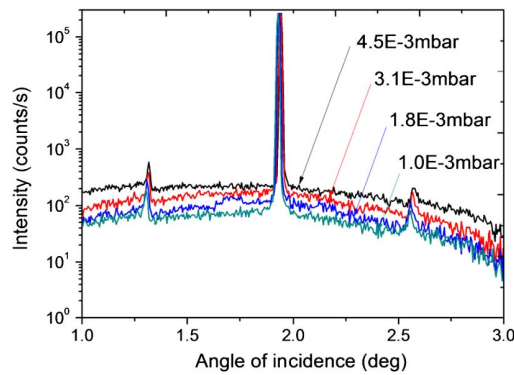


Fig. 2. Diffuse scattering (rocking curves around the third Bragg order) for Mo/Si multilayers deposited with different Ar gas pressures. The decreased intensity indicates that the interface roughness decreases for lower gas pressures.

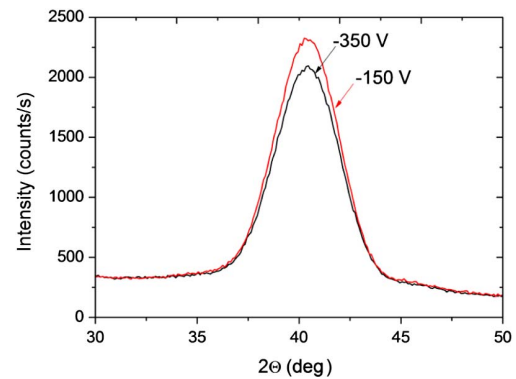


Fig. 4. WAXRD (Mo 110 diffraction peaks) for Mo/Si multilayers deposited with -350 V and -150 V substrate bias. The increased intensity and reduced FWHM indicate that the size of Mo crystallites increases for lower substrate bias voltage.

Table 3. Properties of Samples M3, M5, M6

	Bias	Period		EUV	
		Thickness		Reflectance	Stress
	(V)	(nm)	I'	(%)	(MPa)
M3	-350	6.940	0.37	67.1	-135
M5	-250	6.938	0.37	67.0	-183
M6	-150	6.946	0.38	67.2	-283

influence on the EUV reflectance, whereas it has strong influence on the stress of multilayers. The decrease of substrate bias voltage from -350 V to -150 V results in the increase of stress from -135 MPa to -283 MPa. Figure 3 shows the comparison of diffuse x-ray scattering for Mo/Si multilayers deposited with -350 V and -150 V substrate bias. The increased intensity indicates that the multilayer deposited with lower substrate bias voltage has higher interface roughness. Figure 4 shows the comparison of WAXRD for these two samples. The increased intensity and reduced full width half-maximum (FWHM) of Mo 110 diffraction peaks indicate that the multilayer deposited with lower substrate bias voltage has a larger Mo crystallite size. The little influence of substrate bias on EUV reflectance may be explained by the combined effects of interdiffusion and

interface roughness. The decrease of substrate bias leads to the reduction of the interdiffusion, possibly improving the optical contrast between Mo and Si layers and therefore increasing the EUV reflectance. However, this positive effect on multilayer reflectivity is offset by the increase of interface roughness.

To explain the increase of multilayer stress due to the reduction of substrate bias, a brief description of stress evolution during the growth of the Mo/Si multilayer is helpful. As revealed by Freitag and Clemens [24] using an *in situ* stress measurement tool, the stress development is strongly affected by the interlayer formation and crystallization of Mo. Their result of *in situ* stress measurement during growth of the Mo/Si multilayer is shown in Fig. 5. During the growth of the first few monolayers of Si, i.e., growth of an Si-on-Mo interlayer, there is a large compressive curvature change. After that, the compressive stress relaxes to a constant value similar to the stress measured during growth of the Si single layer film. As soon as the growth of Mo begins, the curvature changes to the tensile direction; this is related to the growth of the Mo-on-Si interlayer. Then, Mo levels off with nearly no curvature changes until the amorphous-to-crystalline transition, which corresponds to an abrupt change of stress. After transition to the crystallization, the stress of Mo becomes compressive. It is

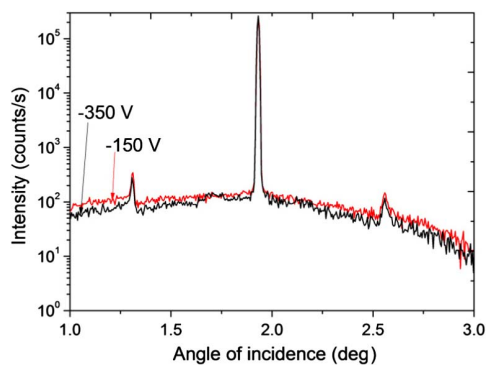


Fig. 3. Diffuse scattering (rocking curves around the third Bragg order) for Mo/Si multilayers deposited with -350 V and -150 V substrate bias. The increased intensity indicates that the interface roughness increases for lower substrate bias voltage.

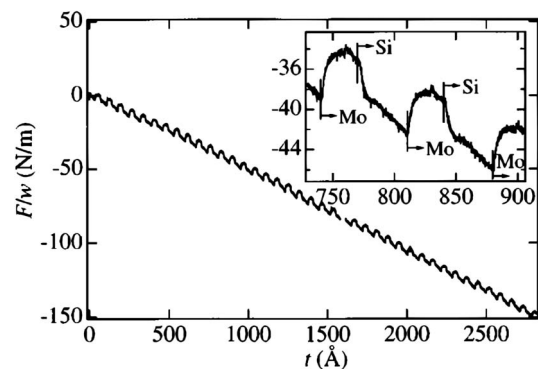


Fig. 5. F/w versus film thickness in a $[40 \times (\text{Si } 41 \text{ Å}/\text{Mo } 28 \text{ Å}) + \text{Si } 41 \text{ Å}]$ multilayer. (Reprinted from Freitag and Clemens [24], with the permission of AIP Publishing. Copyright 1998 AIP Publishing.)

straightforward that ion bombardment of the final part of the Si layer affects the underlying Si-on-Mo interface, and the decrease of substrate bias can reduce the Si-on-Mo interdiffusion. However, this cannot explain the increase of compressive stress with the decrease of substrate bias. As the stress of the Si-on-Mo interlayer is compressive, the reduction of Si-on-Mo interdiffusion should decrease the compressive stress of the Mo/Si multilayer, something not in accordance with the experimental results. Thus, there should be more complicated influences of ion bombardment on the structure of Mo/Si multilayers. As reported by Bajt *et al.* [25], there is a critical thickness at which the Mo layer state changes from amorphous to crystalline during the growth of Mo/Si multilayers, and this behavior can be explained by the fact that the first few monolayers of Mo react with the underlying Si to form the Mo-on-Si interlayer, and Mo crystallization is suppressed until the Si concentration is below the solid solubility limit in the Mo crystal. Thus, the increase of the Mo crystallite size for lower substrate bias voltage may be related not only to reduction of consumed Mo due to the decrease of interlayer formation but also to the reduction of Mo crystallization threshold thickness for lower substrate bias voltage i.e., lower energy of Ar ion bombardment, as explained by Bosgra [26] in the study of the Mo growth on the treated Si surfaces monitored by an *in situ* ellipsometry. For lower energy of Ar ions, the probability is lower to create defects. The reduced defects can increase the cohesive energy of the Si surface atoms, and the increased Si cohesive energy at the surface in turn reduces the probability for Mo-on-Si interdiffusion during deposition. Thus, the decreased energy of Ar ions may reduce not only the Si-on-Mo interdiffusion but also the Mo-on-Si interdiffusion, meaning that the Si concentration reaches a level below the solid solubility limit at a smaller amount of deposited Mo; i.e., the Mo layer starts to crystallize at a smaller amount of deposited Mo. As the stress of the Mo-on-Si interlayer is tensile and the stress of crystallized Mo is compressive, the reduction of the Mo-on-Si interlayer and ahead of crystallization transition can both increase the compressive stress value of the Mo/Si multilayer, contrary to the effect of reducing Si-on-Mo interdiffusion. As shown in the experimental results, the compressive stress of the Mo/Si multilayer deposited with -150 V substrate bias is obviously larger than that of the Mo/Si multilayer deposited with -350 V substrate bias. This indicates that the reduction of Mo-on-Si interdiffusion and ahead of crystallization transition may play a dominant role in affecting the stress in this case.

C. Influence of Bias-Assisted Si Ratio on the Reflectance and Stress

Samples M7 and M8 were produced by varying the ratio of the final part of the Si layer with bias assistance relative to sample M3. The ratios were 25% and 75%, respectively. The properties of these samples are summarized in Table 4. The variation of the ratio has limited influence on the stress, whereas it has remarkable influence on the EUV reflectance of multilayers. Figure 6 shows the comparison of diffuse x -ray scattering for these three samples. The interface roughness does not decrease monotonously with increasing the bias-assisted Si ratio. For 50% of the Si layer deposited with bias, the interface roughness is lowest. For 75% of the Si layer deposited with bias, the

Table 4. Properties of Samples M7, M3, M8

	Assisted Si Ratio	Period Thickness (nm)	Stress (MPa)	EUUV Reflectance (%)	Stress (MPa)
M7	25%	6.887	0.37	68.0	-164
M3	50%	6.940	0.37	67.1	-135
M8	75%	6.890	0.39	64.2	-132

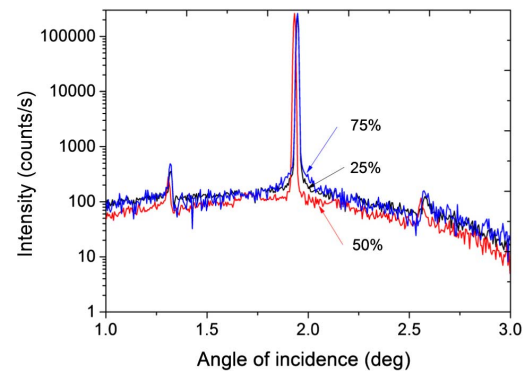


Fig. 6. Diffuse scattering (rocking curves around the third Bragg order) of Mo/Si multilayers for the final 25%, 50%, and 75% of Si deposited with bias assistance.

initial part of the Si layer is too thin and the accelerated Ar ions penetrate through this layer and bombard the underlying Mo crystallites, possibly increasing not only the Si-on-Mo interdiffusion [27] but also the roughness of the Mo layer due to the preferential sputtering [28]. Figure 7 shows the comparison of WAXRD. With the increase of the bias-assisted Si ratio, the Mo crystallite size decreases monotonously. Figure 8 shows the TEM analysis of Mo/Si multilayers with 25% and 75% of the bias-assisted Si layer. The Mo/Si multilayer with 75% of the bias-assisted Si layer has an obviously thicker Si-on-Mo interlayer than the one with 25% of the bias-assisted Si layer. Owing to limited image quality, the difference of the Mo-on-Si interlayer between the two samples is not well-pronounced. Figure 9 shows the comparison of EDX depth profiles of these two samples. The amplitude of the Mo and Si concentration

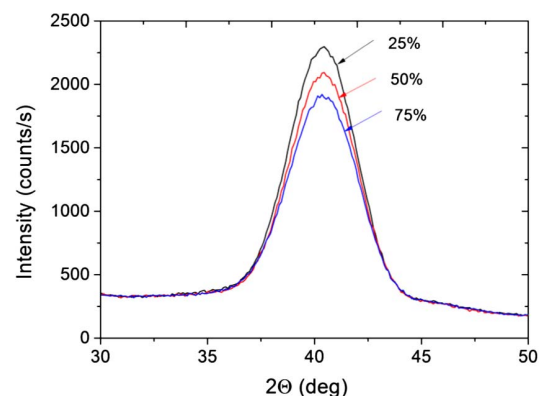


Fig. 7. WAXRD (Mo 110 diffraction peaks) of Mo/Si multilayers for the final 25%, 50%, and 75% of Si deposited with bias assistance.

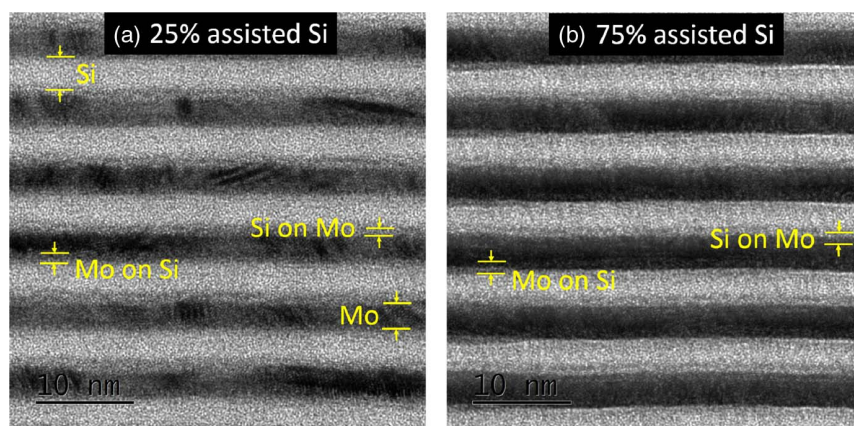


Fig. 8. Cross-sectional HRTEM images of Mo/Si multilayers with (a) 25% and (b) 75% of the bias-assisted Si layer.

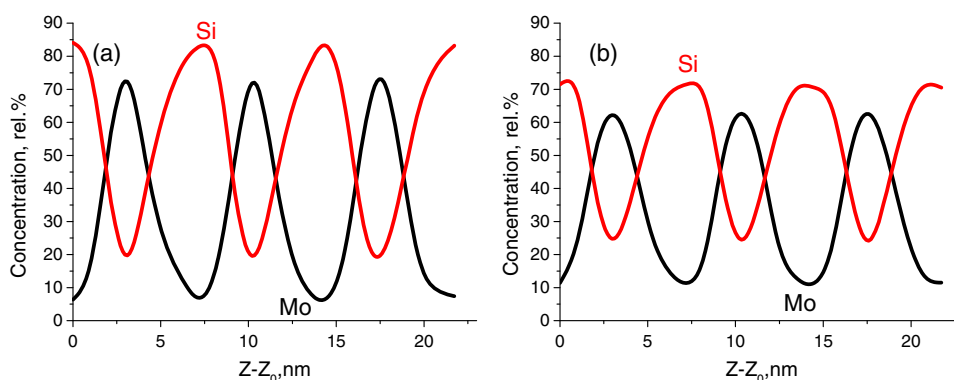


Fig. 9. EDX depth profiles of the relative atomic concentration of the dominant chemical elements composed of Mo/Si multilayers with (a) 25% and (b) 75% of the bias-assisted Si layer.

oscillations decreases with the increase of the bias-assisted Si ratio, demonstrating the decreasing sharpness of the Mo/Si multilayer structure interfaces. A separate comparison of Si relative atomic concentration depth profiles in Fig. 10 shows more clearly that the sharpness of not only the Si-on-Mo interface but also the Mo-on-Si interface is reduced with increasing bias-assisted Si ratio. This is direct evidence that too much bias assistance may not only increase the Si-on-Mo interdiffusion but also the Mo-on-Si interdiffusion. As explained in 3.B, the increase of Mo-on-Si interdiffusion may further lead to the postponement of the Mo crystallization transition, one reason for the decrease of Mo crystallite size. The increase of interdiffusion, along with the decrease of Mo crystallite size, can contribute to the reduction of the optical contrast of Mo/Si multilayers. The monotonous decrease of EUV reflectance with the increasing bias-assisted Si ratio indicates that this reduction of optical contrast has a dominant effect on the EUV reflectance.

It is worthwhile to discuss the difference between the effect of reducing bias voltage and that of reducing the bias-assisted Si ratio relative to the sample M3. The reduction of bias voltage to -150 V did not further improve the EUV reflectance. Moreover, it resulted in an obvious increase of compressive stress. The reduction of the bias-assisted Si ratio to 25%

increased the peak reflectance by nearly 1% with increasing the stress by only 29 MPa. The diffuse scattering and WAXRD show that the multilayer samples prepared under the two above conditions have close interface roughness and Mo crystallite size, implying that the difference of EUV reflectance and stress between them may be correlated to the difference of Si-on-Mo interdiffusion. The reduction of the bias-assisted Si ratio and thereby the increase of thickness of the initial Si layer without bias assistance may perform better

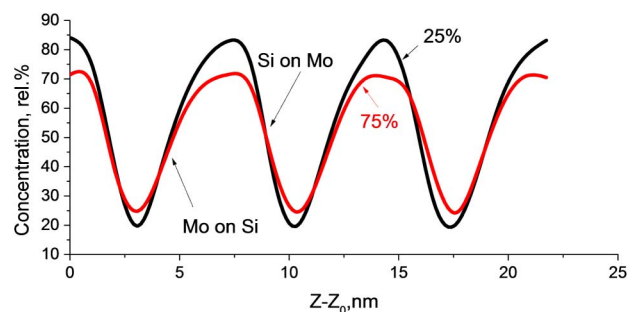


Fig. 10. Comparison of the Si relative atomic concentration depth profiles between Mo/Si multilayers with 25% and 75% of the bias-assisted Si layer.

in reducing the Si-on-Mo interdiffusion, something critical to obtain low-stress and high-reflectance Mo/Si multilayers.

4. CONCLUSION

In this study, we explored the potentiality of achieving low-stress and high-reflectance Mo/Si multilayers by conventional magnetron sputtering deposition with bias assistance. As the stress of the Si-on-Mo interlayer is compressive, the first rule to relieve the large compressive stress of Mo/Si multilayers while retaining high EUV reflectance is to reduce the Si-on-Mo interdiffusion while keeping a relatively low interface roughness. Therefore, in this research only the final part of the Si layer was deposited with bias assistance. The interface roughness of Mo/Si multilayers decreases with decreasing Ar gas pressure. However, too much reduction of Ar gas pressure may increase the interdiffusion, unfavorable for achieving high reflectance. The Si-on-Mo interdiffusion can be reduced by the reduction of bias voltage or the reduction of the bias-assisted Si ratio. The experimental results indicate that the latter may be more efficient in reducing the Si-on-Mo interdiffusion.

Funding. National Natural Science Foundation of China (NSFC) (61605201).

REFERENCES

1. D. Stearns, R. Rosen, and S. Vernon, "Fabrication of high-reflectance Mo-Si multilayer mirrors by planar-magnetron sputtering," *J. Vac. Sci. Technol. A* **9**, 2662–2669 (1991).
2. S. Bajt, J. B. Alameda, T. W. Barbee, Jr., W. M. Clift, J. A. Folta, B. B. Kaufmann, and E. A. Spiller, "Improved reflectance and stability of Mo/Si multilayers," *Proc. SPIE* **41**, 65–75 (2001).
3. Y. Li, H. Zhang, H. Wang, F. He, X. Wang, Y. Liu, S. Han, X. Zheng, X. Wang, and B. Chen, "Thermal and stress studies of the 30.4 nm Mo/Si multilayer mirror for the moon-based EUV camera," *Appl. Surf. Sci.* **317**, 902–907 (2014).
4. D. Voronov, E. Anderson, E. Gullikson, F. Salmassi, T. Warwick, V. Yashchuk, and H. Padmore, "Control of surface mobility for conformal deposition of Mo-Si multilayers on saw-tooth substrates," *Appl. Surf. Sci.* **284**, 575–580 (2013).
5. B. Schmiedeskamp, A. Kloidt, H.-J. Stock, U. Kleineberg, T. Doehring, M. Proepper, S. Rahn, K. Hilgers, B. Heidemann, and T. Tappe, "Electron-beam-deposited Mo/Si and Mo/Si/Si multilayer x-ray mirrors and gratings," *Opt. Eng.* **33**, 1314–1321 (1994).
6. E. Louis, A. E. Yakshin, P. C. Goerts, S. Abdali, E. L. Maas, R. Stuik, F. Bijkerk, D. Schmitz, F. Scholze, and G. Ulm, "Reflectivity of Mo/Si multilayer systems for EUVL," *Proc. SPIE* **3676**, 844–845 (1999).
7. E. Spiller, S. L. Baker, P. B. Mirkarimi, V. Sperry, E. M. Gullikson, and D. G. Stearns, "High-performance Mo-Si multilayer coatings for extreme-ultraviolet lithography by ion-beam deposition," *Appl. Opt.* **42**, 4049–4058 (2003).
8. P. Kearney, C. Moore, S. Tan, S. Vernon, and R. Levesque, "Mask blanks for extreme ultraviolet lithography: ion beam sputter deposition of low defect density Mo/Si multilayers," *J. Vac. Sci. Technol. B* **15**, 2452–2454 (1997).
9. S. Braun, R. Dietsch, M. Haidl, T. Holz, H. Mai, S. Müllender, and R. Scholz, "Mo/Si-multilayers for EUV applications prepared by pulsed laser deposition (PLD)," *Microelectron. Eng.* **57**, 9–15 (2001).
10. R. Soufli, S. Bajt, R. M. Hudyma, and J. S. Taylor, "Optics and multilayer coatings for EUVL systems," in *EUV Lithography* (SPIE, 2009), Vol. **178**, p. 133.
11. T. Feigl, S. Yulin, T. Kuhlmann, and N. Kaiser, "Damage resistant and low stress EUV multilayer mirrors," *Jpn. J. Appl. Phys.* **41**, 4082–4085 (2002).
12. P. B. Mirkarimi and C. Montcalm, "Advances in the reduction and compensation of film stress in high-reflectance multilayer coatings for extreme-ultraviolet lithography," *Proc. SPIE* **3331**, 133–148 (1998).
13. P. A. Spence, M. P. Kanouff, and A. K. Ray-Chaudhuri, "Film-stress-induced deformation of EUV reflective optics," *Proc. SPIE* **3676**, 724–734 (1999).
14. P. B. Mirkarimi, "Stress, reflectance, and temporal stability of sputter-deposited Mo/Si and Mo/Be multilayer films for extreme ultraviolet lithography," *Opt. Eng.* **38**, 1246–1259 (1999).
15. M. Shiraishi, N. Kandaka, and K. Murakami, "Low-stress and high-reflectivity molybdenum/silicon multilayers deposited by low-pressure rotary magnet cathode sputtering for EUV lithography," *Proc. SPIE* **5374**, 104–111 (2004).
16. R. Soufli, J. Robinson, M. Fernández-Perea, E. Spiller, N. Brejnholt, M.-A. Descalle, M. Pivovarov, and E. Gullikson, "Recent advances in multilayer reflective optics for EUV/x-ray sources," *Springer Proc. Phys.* **169**, 331–337 (2016).
17. A. E. Yakshin, R. W. E. Van De Kruijs, I. Nedelcu, E. Zoethout, E. Louis, F. Bijkerk, H. Enkisch, and S. Müllender, "Enhanced reflectance of interface engineered Mo/Si multilayers produced by thermal particle deposition," *Proc. SPIE* **6517**, 65170I (2007).
18. S. P. Vernon, D. G. Stearns, and R. S. Rosen, "Ion-assisted sputter deposition of molybdenum-silicon multilayers," *Appl. Opt.* **32**, 6969–6974 (1993).
19. E. Zubarev, V. Kondratenko, V. Sevryukova, S. Yulin, T. Feigl, and N. Kaiser, "The structure of Mo/Si multilayers prepared in the conditions of ionic assistance," *Appl. Phys. A* **90**, 705–710 (2008).
20. V. Rigato, A. Patelli, G. Maggioni, G. Salmaso, V. Mattarello, M. G. Pelizzo, P. Nicolosi, L. Depero, E. Bontempi, and P. Mazzoldi, "Effects of ion bombardment and gas incorporation on the properties of Mo/a-Si: H multilayers for EUV applications," *Surf. Coat. Technol.* **174**, 40–48 (2003).
21. G. G. Stoney, "The tension of metallic films deposited by electrolysis," *Proc. R. Soc. London A* **82**, 172–175 (1909).
22. D. Windt, W. Brown, C. Volkert, and W. Waskiewicz, "Variation in stress with background pressure in sputtered Mo/Si multilayer films," *J. Appl. Phys.* **78**, 2423–2430 (1995).
23. Y. P. Pershyn, E. M. Gullikson, V. V. Kondratenko, V. V. Mamon, S. A. Reutskaya, D. L. Voronov, E. N. Zubarev, I. A. Artyukov, and A. V. Vinogradov, "Effect of working gas pressure on interlayer mixing in magnetron-deposited Mo/Si multilayers," *Opt. Eng.* **52**, 095104 (2013).
24. J. Freitag and B. Clemens, "Stress evolution in Mo/Si multilayers for high-reflectivity extreme ultraviolet mirrors," *Appl. Phys. Lett.* **73**, 43–45 (1998).
25. S. Bajt, D. G. Stearns, and P. A. Kearney, "Investigation of the amorphous-to-crystalline transition in Mo/Si multilayers," *J. Appl. Phys.* **90**, 1017–1025 (2001).
26. J. Bosgra, "Interlayer thermodynamics in nanoscale layered structures for reflection of EUV radiation," Ph.D. dissertation (University of Twente, 2013).
27. I. Nedelcu, R. van de Kruijs, A. Yakshin, F. Tichelaar, E. Zoethout, E. Louis, H. Enkisch, S. Müllender, and F. Bijkerk, "Interface roughness in Mo/Si multilayers," *Thin Solid Films* **515**, 434–438 (2006).
28. R. Schlatmann, C. Lu, J. Verhoeven, E. Puik, and M. van der Wiel, "Modification by Ar and Kr ion bombardment of Mo/Si X-ray multilayers," *Appl. Surf. Sci.* **78**, 147–157 (1994).